THE ASTROPHYSICAL JOURNAL, 266:28–40, 1983 March 1

PROMINENT ULTRAVIOLET EMISSION LINES FROM TYPE 1 SEYFERT GALAXIES

CHI-CHAO WU[1]
Computer Sciences Corporation
AND
ALBERT BOGGESS[1] AND THEODORE R. GULL[1]
Laboratory for Astronomy and Solar Physics, NASA Goddard Space Flight Center
Received 1982 May 6; accepted 1982 August 24

ABSTRACT

New data obtained at about 6 Å resolution with the *International Ultraviolet Explorer* satellite are reported for Lyα, C IV λ1550, C III] λ1909, Mg II λ2800, and the continuum at 1450 Å for 20 Seyfert galaxies and one quasar. The fluxes of these lines correlate well with the continuum flux at 1450 Å indicating that photoionization is the dominant heating mechanism for these active galactic nuclei. The observed Lyα/Hβ ratio is about 5. Combining the data for Seyferts and high redshift quasars which cover five orders of magnitude in continuum luminosity, lower luminosity objects have higher equivalent widths for their emission lines. This suggests that the covering factor increases with decreasing luminosity. The C IV/C III] ratio is about 2 for high z quasars and 5 for type 1 Seyferts, indicating that Seyfert 1 galaxies have higher ionization parameters. The line ratios predicted by the Kwan and Krolik model are found to be in good agreement with those observed for type 1 Seyferts which have C IV/C III] ratio between 3.5 and 6.5.

The continuum spectrum between 10 μm and 1200 Å is steeper than the power law for the 2–60 keV region. Between the Lyman limit and 2 keV, the extrapolation of the IR-UV spectrum falls significantly above that of the X-rays. Therefore, a simple extrapolation of the optical spectrum may grossly overestimate the amount of ionizing photons.

Subject headings: galaxies: Seyfert — quasars — ultraviolet: spectra

I. INTRODUCTION

In recent years significant amounts of observational data have become available for Seyfert galaxies. For example: reported data include papers by de Bruyn and Wilson (1976) in the radio, Rieke (1978) and Lacy *et al.* (1981) in the infrared, Osterbrock (1977), Osterbrock and Shuder (1981), and de Bruyn and Sargent (1978) in the optical, and Mushotzky *et al.* (1980) and Lawrence and Elvis (1981) in the X-rays. Since the launch of the *International Ultraviolet Explorer* (*IUE*), we have observed 20 Seyferts. Earlier, we reported the H I Lyα fluxes (Wu, Boggess, and Gull 1980) and the C IV λ1550 emission-line profile (Wu, Boggess, and Gull 1981). Additionally, results of nine other Seyferts were also published by other investigators (see references to Table 1). In this investigation, we will give the measured fluxes and equivalent widths of the four strongest emission lines, Lyα, C IV λ1550, C III] λ1909, and Mg II λ2800 and the observed continuum flux at the rest wavelength 1450 Å from the 29 Seyferts. For convenience, we also include the results for the low redshift quasar MR 2251-178. Measurements of other emission and absorption lines for the 21 objects we observed and the more complete presentation of their spectral data will be given in our next paper (Wu, Boggess, and Gull 1982). The ultraviolet data provide an important complement to the wealth of observational material already available at other wavelength regions. Hence, more complete and detailed studies of the Seyfert phenomena can be carried out. Furthermore, the UV data for Seyfert galaxies can be compared with those of high redshift quasars measured in a consistent manner by Baldwin (1977*b*), Osmer and Smith (1980), or by the Michigan group (Lewis, MacAlpine, and Weedman 1979; MacAlpine and Feldman 1982) in order to investigate if and how these two types of active galaxies differ from each other.

Since the pioneering work of Davidson (1972) and MacAlpine (1972) in the theoretical modeling of active galactic nuclei, computations of increasing sophistication are becoming available (Davidson and Netzer 1979; Canfield and Puetter 1981; Kwan and Krolik 1981). With the availability of spectral data in the IR, optical, UV, and the X-rays (unfortunately the observations were not made at the same time) for individual Seyferts, realistic models can be computed for individual objects instead of having to base the computations on the "representative spectrum" of quasars. Since different

[1] Guest Investigator of the *IUE* Observatory, operated by Goddard Space Flight Center, National Aeronautics and Space Administration.

Seyferts (and quasars) may show rather diverse line ratios, the advantage of making models for single objects is obvious. This has been attempted by Ferland and Mushotzky (1982) for NGC 4151.

II. OBSERVATIONS AND RESULTS

Observations were made with the short wavelength prime (SWP) and the long wavelength redundant (LWR) cameras on board the *International Ultraviolet Explorer* (*IUE*) satellite. The SWP camera covers the spectral region between 1150 and 2000 Å and, in low dispersion mode, has a resolution of about 5 Å. The LWR covers the 1900–3200 Å spectral region with a resolution of about 8 Å. More details on the *IUE* scientific instruments and their performance are given in Boggess *et al.* (1978*a*, *b*).

As indicated in Table 1, new data are reported here for 21 objects while the data for the remaining nine are results published by other investigators. For these nine objects, we refer the readers to the original literature for observational details. For the 21 objects observed by us and our collaborators, the data for I Zw 1, NGC 1068, Mrk 78, NGC 4593, Mrk 478, II Zw 136, and NGC 7213 were obtained by taking a single spectrum through the $10'' \times 20''$ aperture. The remaining 14 objects were observed with the pseudotrail technique first used by Wu, Boggess, and Gull (1981) for line profile studies. With this technique, three spectra were taken side by side in the $10'' \times 20''$ aperture along the axis perpendicular to the direction of dispersion. A significant improvement in the signal-to-noise ratio is achieved by the pseudotrail spectra because there is a factor of 3 increase in the number of photons collected without reaching saturation. Also, with the spectra spread over 3 times more pixels, therefore, the readout noise associated with individual pixels is more likely to be averaged out.

For galaxies with redshift less than 3000 km s^{-1}, the geocoronal Lyman-α photons scattered into the large aperture severely contaminate the Lyα emission from the Seyferts. In principle, the smaller 3″ diameter can be used. But it may miss the point source Seyfert nucleus, it lengthens the exposure time by at least a factor of 2, and it does not give the absolute value of the fluxes. For these reasons, the Lyα fluxes for most of the NGC objects are not available. NGC 4151 is bright; a 15 minute exposure taken when the Earth was sufficiently far away in the sky allows the Lyα flux to be measured with negligible contamination. An exposure for NGC 3783 was taken through the 3″ aperture; the blue half of the Lyα emission is found to be severely absorbed, probably by gas in our Galaxy because strong absorption lines of O I λ1304, C II λ1335, Si IV λ1400, Fe II λ1608, Fe II λ2600, Mg II λ2800 (strongly blended with the component from the broad-line clouds), and Mg I λ2852 are present near the zero redshift. Adopting the ground measured $cz = 2740$ km s^{-1} (Weedman 1977), the line center for Lyα is then 1227 Å. We assume the Lyα flux and equivalent width are twice the value measured for $\lambda \geq 1227$ Å. We are planning to publish all our original data in another paper (Wu, Boggess, and Gull 1982), we will defer more detailed discussion of observations to that paper.

The data were processed by the *IUE* observatory staff. Except for 3C 120 and Mrk 79, all SWP data either have been corrected for or are free of the effects of the erroneous intensity transfer function (ITF) being used between 1978 May 22 and 1979 July 7 (see Holm 1979). The absolute calibration of Bohlin and Holm (1980) was adopted to establish the flux level for the spectra obtained by ourselves. No attempt was made to correct the measurements by the other investigators to the Bohlin-Holm system, because earlier calibration by Bohlin and Snijders (1978) and Bohlin *et al.* (1980) do not differ significantly from it (generally $\lesssim 12\%$). Fluxes of the emission lines were measured from 50 Å per inch plots with a planimeter. The continuum level for SWP was established by adopting the windows having the following central wavelengths and full widths (in parentheses): 1345 Å (50 Å), 1450 Å (50 Å), 1700 Å (30 Å), and 1790 Å (60 Å) (see Wu, Boggess, and Gull 1981). For LWR, the continuum windows at 1990(60), 2665(50), and 2910(30) were adopted.

The combined short and long wavelength (SWP + LWR) spectra of four Seyfert galaxies are shown in Figure 1. The strong geocoronal Lyα emission which contaminates all long-exposure SWP images from 1203 to 1226 Å has been omitted from the plots. In the Mrk 279 spectrum, note the Lyα and the C IV λ1550 absorption lines shortward of their respective emission line peaks. Similar absorption is also present in Mg II λ2800. These lines are probably caused by a broad line cloud along the line of sight. Absorption lines originated in or near our own Galaxy are present in all four spectra. The four strongest emission lines are H I Lyα, C IV λ1550, C III] λ1909, and Mg II λ2800 from the Seyferts. The strength of these lines are tabulated in Table 1. The first three columns give, respectively, a running number associated with each object, the name of the object and the year and day number of observation. The next four columns present the observed flux on the first line and the observed equivalent width on the second line for the Lyα, C IV, C III] and Mg II emission. The eighth column gives the observed continuum flux in ergs cm^{-2} s^{-1} $Å^{-1}$ at the rest wavelength of 1450 Å. The columns headed Hβ and Hα/Hβ are Balmer line measurements from the sources given in the reference column; mostly they are derived from the equivalent widths of Osterbrock (1977) and the continuum fluxes of de Bruyn and Sargent (1978) as explained in Wu, Boggess, and Gull (1980). The column headed H_x gives the X-ray luminosity as defined in Lawrence and Elvis (1981). The last column gives the sources of UV and optical measurements.

III. DISCUSSION

a) Emission Line—Continuum Correlation

It is generally accepted that the gas associated with the active galactic nuclei is heated by the photoionization

TABLE 1

OBSERVED FLUXES, EQUIVALENT WIDTHS, AND LINE RATIOS OF SEYFERT GALAXIES

		Year/Day	Flux (ergs cm^{-2} s^{-1}) / Equivalent Width (Å) L_α	C IV	C III]	Mg II	f_λ(1450)	H_β	H_α/H_β	H_x	References
1	Mrk 335	81/45	1.06E-11 212.0	3.68E-12 92.0	5.80E-13 19.0	5.01E-13 22.4	4.30E-14	1.15E-12	2.60	43.89	1,2,3
2	III Zw 2	81/159,153	1.30E-12 141.3	8.94E-13 116.1	2.47E-13 48.6	2.61E-13 35.5	8.15E-15	6.77E-13	3.58	45.08	1,2,3
3	I Zw 1	79/163	2.51E-12 304.5	6.87E-13 72.4		6.11E-13 49.3	9.00E-15	4.17E-13	4.86	44.26[a]	1,2,3
4	Fairall 9	81/153	1.87E-11 187.0	7.31E-12 84.5	1.45E-12 29.1	1.95E-12 55.2	9.35E-14	2.20E-12	2.51	44.38	1,4,5
5	NGC 985	81/220	2.42E-12 180.8	1.70E-12 153.5	4.62E-13 47.9	6.21E-13 84.0	1.18E-14	3.51E-13	3.48	43.93[b]	1,6
6	NGC 1068	80/175		5.49E-12 89.7	2.20E-12 40.4	1.17E-12 21.3	6.36E-14	1.6 E-12	4.47	43.03[a]	1,7
7	NGC 1566	79/221		5. E-13	2.5 E-13			1.6 E-13	4.00		8
8	3C 120	78/104 78/324	1.78E-12 81	3.58E-12 291	6.9 E-13 88	1.12E-12 91	1.23E-14[c]	3.7 E-13	5.1	44.43	9
9	Akn 120	81/218	7.05E-12 141.0	4.22E-12 91.6	7.33E-13 20.7	1.52E-12 47.4	4.98E-14	1.1 E-12	3.90	43.96	1,10,11
10	Mrk 3	79/225	4.8 E-13	2.3 E-13	1.0 E-13	2. E-13		2.1 E-13	5.31		8,7
11	Mrk 9	78/326,324	2.44E-12 124	9.7 E-13 62		2.3 E-13 26	1.6 E-14[c]	3.0 E-13	3.7	43.8[a]	12
12	Mrk 78	79/20	4.96E-13 258.20				1.47E-15	2.2 E-14	5.31	43.0[a]	1.7
13	Mrk 79	78/105	2.14E-12 66	1.98E-12 91	4.7 E-13 36	2.6 E-13 24	2.18E-14[c]	9.6 E-13	4.7	43.8	9
14	Mrk 10	78/333, 80/37	1.12E-12 161	7.1 E-13 109		3.1 E-13 50	6.51E-15[c]	2.9 E-13	2.4		12
15	NGC 3783	81/221	1.07E-11[d] 207.8	7.36E-12 163 6	5.92E-13 15.2	1.55E-12 49.7	4.71E-14	7.70E-13	3.38	43.28	1,13
16	NGC 4151	79/341 79/347	3.09E-11 220.4	3.68E-11 248.5	4.67E-12 42.8	4.34E-12 60.4	1.57E-13	6.22E-12	2.91	42.88	1,14
17	NGC 4593	79/365		1.74E-12 189.0	2.90E-13 33.3	7.40E-13 77.1	9.10E-15	6.98E-13	2.61		1,15
18	Mrk 231	78/356,350	3.4 E-13:			1.7 E-13:		3.4 E-13			16,17
19	Mrk 279	81/160,269	4.22E-12 156.3	2.87E-12 121.9	2.84E-13 21.7	9.48E-13 68.2	2.43E-14	1.00E-12	2.89	44.27	1,2,3
20	NGC 5548	79/342 79/347	1.00E-11 147.6	6.81E-12 108.0	1.23E-12 25.8	1.85E-12 57.6	6.85E-14	1.27E-12	4.21	43.68	1,2,3
21	Mrk 478	78/190,184 78/244	3.88E-12 158.5	8.37E-13 34.3	3.66E-13 24.1	2.07E-13 20.9	2.33E-14	3.31E-13	4.32		1,2,3
22	3C 390.3	78/326	1.54E-12[e] 6.55	7.4 E-13[e] 470		3.0 E-13 165	1.7 E-15[c]	2.6 E-13	6.3	44.69	12
23	ESO 141-G55	81/69	1.04E-11 116.9	5.36E-12 76.0	1.12E-12 29.6	1.53E-12 45.0	7.55E-14	1.20E-12	3.67	44.08	1,4
24	Mrk 509	79/340	1.13E-11 188.6	6.75E-12 132.3	1 38E-12 38.2	2.07E-12 65.1	5.38E-14	2.18E-12	2.83	44.39	1,2,3
25	II Zw 136	78/184	3.09E-12 130.9	1.13E-12 55.9	6.25E-13 48.5	3.30E-13 29.2	2.14E-14	6.86E-13	3.63		1,2,3
26	NGC 7213	80/265,277		1.29E-12 134.4	6.79E-13 102.8		1.05E-14			42.46[b]	1
27	NGC 7469	79/365	5.95E-12 136.8	3.80E-12 94.2	6.25E-13 16.9	1.33E-12 46.6	4.13E-14	1.91E-12	3.88	43.83	1,2,3
28	MR 2251-178[f]	81/102	1.02E-11 656.5	3.60E-12 270.5	3.34E-13 55.3	7.15E-13 73.0	1.35E-14	6.7 E-13	4.27	44.91	1,18
29	MCG-2-58-22	79/353	6.68E-12 167.0	5.10E-12 164.5		1.30E-12 82.5	3.38E-14	1.72E-12	2.68	44.74	1,4
30	NGC 7603	79/311	3. E-13	1. E-13				4.82E-14			8

[a] Converted to H_x from the measured S_x and H_x-S_x relationship given in Fig. 4 of Lawrence and Elvis 1982.

[b] *HEAO 1* measurements; R. F. Mushotzky 1980, private communication.

[c] Estimated from the observed fluxes and equivalent widths of C IV λ1550, $f_\lambda(1450)$ = flux (C IV)/eq. width (C IV).

[d] Blue half of Lyα is heavily absorbed. The Lyα flux and equivalent width are estimated by setting them equal to twice the value measured for the red half of the line.

[e] Combined values for the broad and narrow components.

[f] A QSO.

REFERENCES.—(1) This investigation. (2) Osterbrock 1977. (3) de Bruyn and Sargent 1978. (4) Ward *et al.* 1978. (5) Hawley and Phillips 1978. (6) Osterbrock 1980. (7) Koski 1978. (8) Schleicher, Fricke, and Kollatschny 1980. (9) Oke and Zimmerman 1979. (10) Peterson 1982. (11) Osterbrock and Phillips 1977. (12) Oke and Goodrich 1981. (13) Osmer, Smith, and Weedman 1974. (14) Anderson 1970. (15) MacAlpine, Williams, and Lewis 1979. (16) Snijders *et al.* 1980. (17) Boksenberg *et al.* 1977. (18) Canizares, McClintock, and Ricker 1978.

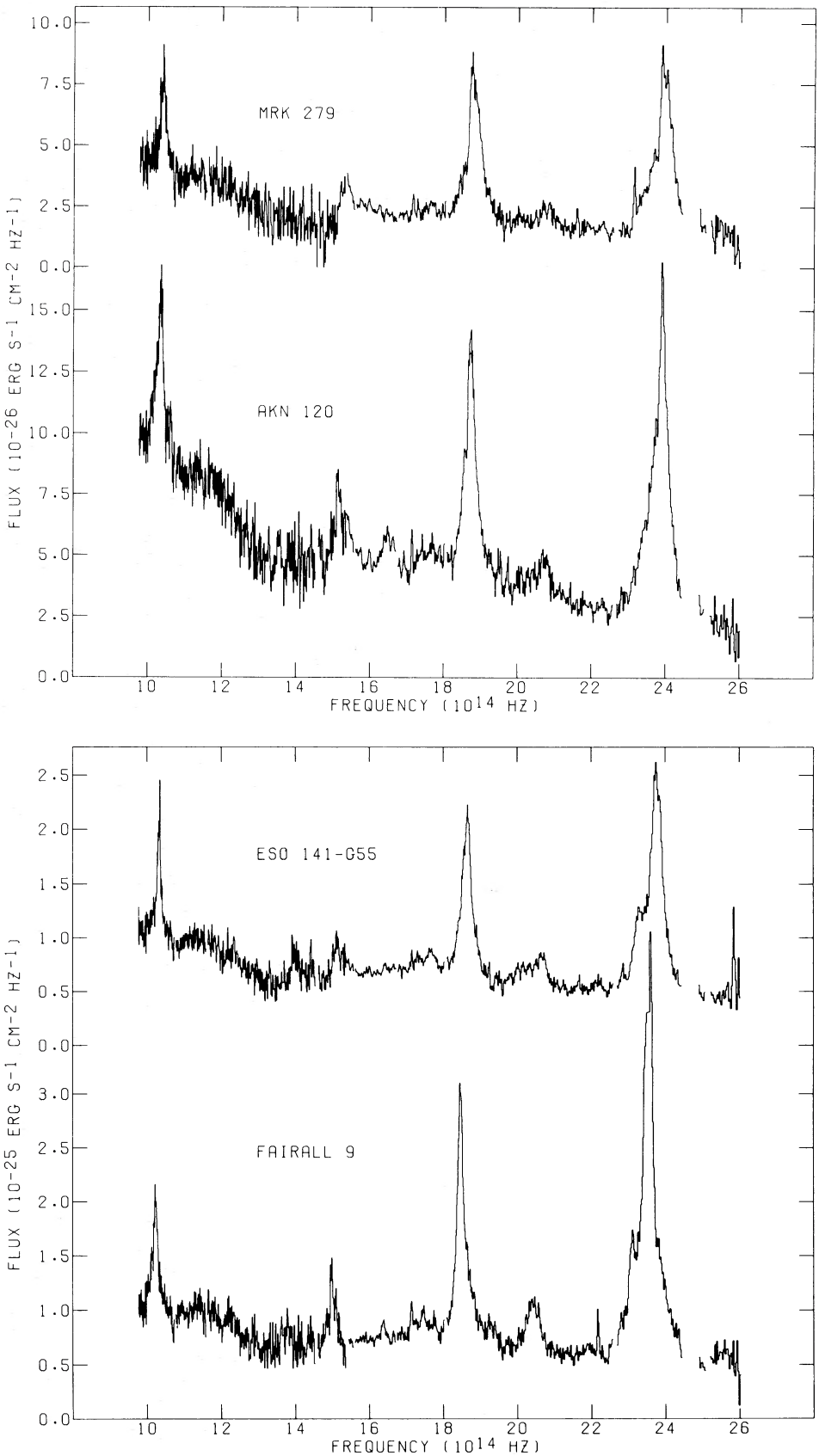

FIG. 1.—*IUE* low-dispersion spectra of (*a*) Mrk 279 and Akn 120 and (*b*) ESO 141−G55 and Fairall 9. Both the flux and the frequency are plotted in their observed values. The 1203–1226 Å region which is contaminated by the geocoronal Lyα and the wavelengths affected by reseau marks are not plotted. It is evident that the LWR camera is intrinsically more noisy than the SWP.

process with the power-law continuum providing the ionizing photons. The good correlation between optical emission-line intensities and the nonthermal continuum at 4800 Å (Shuder 1981) and the near constancy of the Balmer line equivalent widths from the active galaxies (Adams and Weedman 1975; Osterbrock 1978) strongly support this photoionization hypothesis. Figures 2*a*–2*d* show the correlation between the observed fluxes of Lyα, C IV λ1550, C III] λ1909, and Mg II λ2800 and the observed monochromatic continuum flux at 1450 Å. The radio-quiet Seyfert 1 galaxies and the Seyfert 2 galaxy Mrk 78 form a tight correlation between Lyα and $f_\nu(1450)$. Significantly removed from this correlation are the broad line radio galaxy (BLRG) 3C 390.3 and the quasar MR 2251−178. As shown in Figures 2*b*–2*d* also, the BLRG and QSO tend to have stronger emission lines for the same continuum level. The implication of this will be discussed in § III*c*. The correlations for the C IV, C III] and Mg II lines show larger scatter than that for Lyα. The small scatter in the Lyα cor-

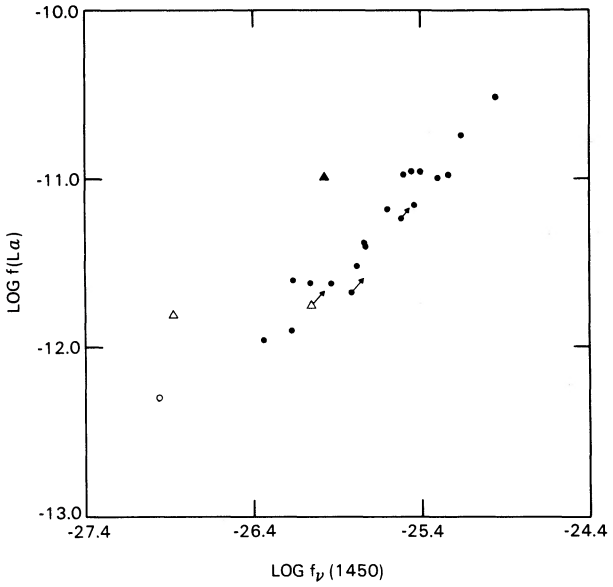

FIG. 2*a*

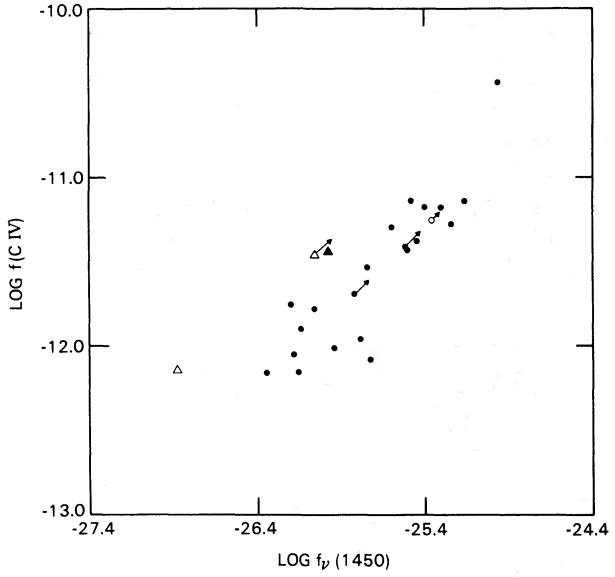

FIG. 2*b*

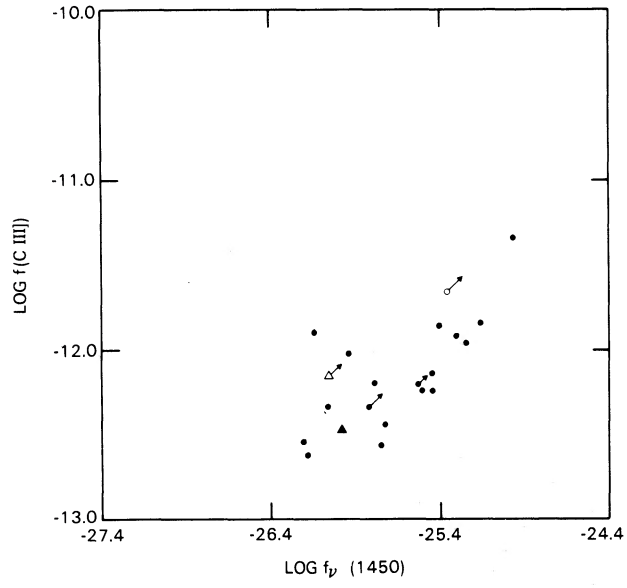

FIG. 2*c*

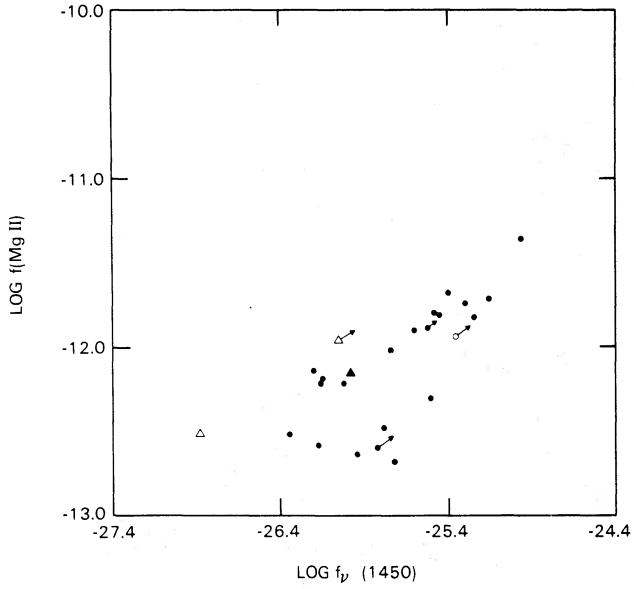

FIG. 2*d*

FIG. 2.—The correlation between the observed monochromatic continuum flux at 1450 Å and the observed flux for (*a*) H I Lyα, (*b*) C IV λ1550, (*c*) C III] λ1909, and (*d*) Mg II λ2800. *Filled circles:* type 1 Seyferts; *open circle:* type 2 Seyferts, Mrk 78 for Lyα and NGC 1068 for the other three lines; *filled triangle:* quasar—in this plot it is MR 2251−178; *open triangles:* broad line radio galaxies 3C 120 and 3C 390.3. The arrows indicate the direction of reddening correction. The length of the arrows is arbitrary.

relation maybe is another observational evidence that, because of its large optical depth, Lyα emission by the broad line clouds has reached its Planck limit as suggested by Zirin (1978). Or it may simply be due to the fact that Lyα arises largely from recombination of the most abundant ion in the H II zone of the BLCs, while the other three lines are collisionally excited and scatter can be introduced by the different physical conditions in the BLR (e.g., as a result of different ionization parameters) of the objects. For C III] λ1909, contributions from Si III] λ1892 may be also cause additional scatter.

In Figure 3, we plot the correlations between the luminosity of C IV λ1550 and continuum luminosity at 1450 Å and in the 2–10 keV band. The plots include quasars, broad line radio galaxies, Seyfert 1 galaxies, and the type 2 Seyfert NGC 1068. They cover four orders of magnitude in luminosities. The good correlation between the strength of the UV emission lines and the level of the UV and X-ray continuum (Figs. 2 and 3) provides further support that the nonthermal continuum is the source for heating the gas associated with the active galaxies.

Taking into account the fact that the X-ray and UV observations were made at different epochs, the correlation in Figure 3 between C IV and the X-rays may be considered as good as that between C IV and the continuum at 1450 Å. This indicates that the optical–X-ray spectrum is very similar among Seyfert galaxies. The similarity of the X-ray spectrum for Seyfert galaxies has already been reported by Mushotzky *et al.* (1980). Figure 4 shows the optical–X-ray spectra of two Seyfert 1 galaxies. Plots of other galaxies for which Mushotzky *et al.* (1980) have X-ray spectra show that indeed their continuum shape from 10 μm to 10 keV do not deviate significantly from one another. This is manifested in the small range for the ratio of the X-ray luminosity (the eleventh column) and the monochromatic luminosity at 1450 Å (derived from the eighth column). For 15 type 1 Seyferts, L_x/L_ν (1450) = 1.6×10^{15} Hz. Except for Fairall 9 and ESO 141-G55 which have L_x/L_ν (1450) $\sim 4 \times 10^{14}$ and III Zw 2, for which the ratio is 5.6×10^{15}, all other objects have the ratio within a factor of 2 of the average value. Not included in the averaging are 3C 120, Mrk 79, and NGC 7469 because of the uncertainty in their large reddening correction at 1450 Å and 3C 390.3 which has the extremely high ratio of L_x/L_ν (1450) = 2.8×10^{16} Hz. For QSOs, the ratio for 3C 273 and MR 2251−178 are 6.8×10^{14} and 3.4×10^{15} Hz, respectively.

Without detailed fitting, we can qualitatively state that the optical power law (10 μm to 1200 Å) is significantly steeper than the X-ray power law. However, in the critical region between the Lyman limit and 2 keV the extrapolation of the optical power law lies well above the extrapolation of the X-ray spectra. Therefore, a simple extrapolation of the optical spectrum may lead to gross overestimate of the number of photons available for heating. In order to join up with the X-ray

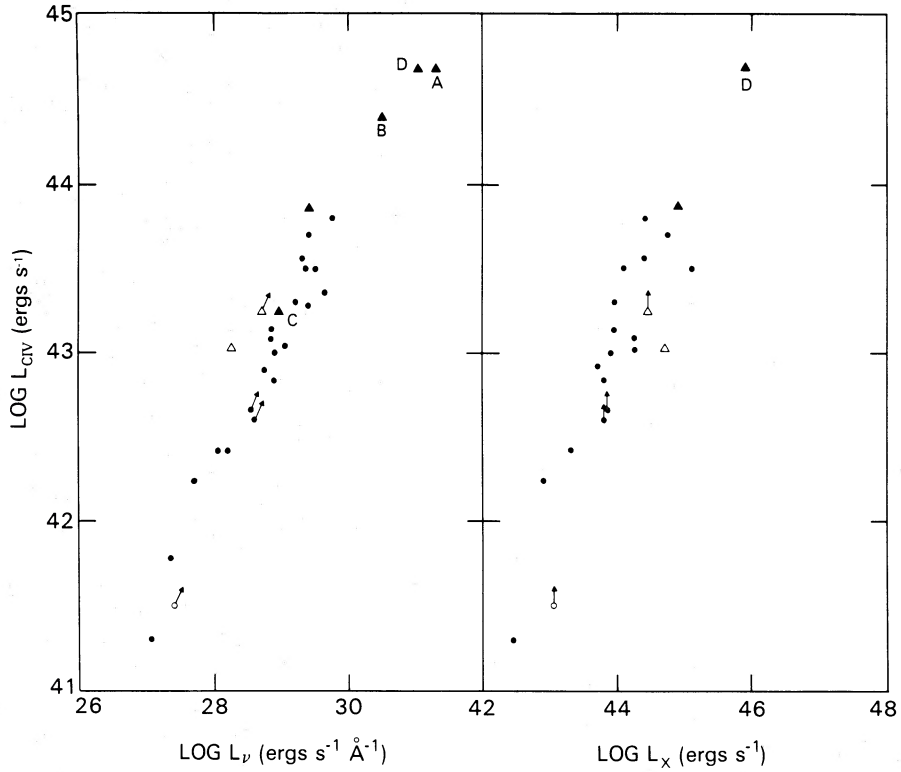

FIG. 3.—The correlation between the C IV λ1550 luminosity and the luminosity at 1450 Å and 2–10 keV. The symbols have the same meaning as in Fig. 2. The four other quasars observed by the *IUE* are A: PKS 0405−123; B: PG 0953+415; C: Mrk 205; and D: 3C 273.

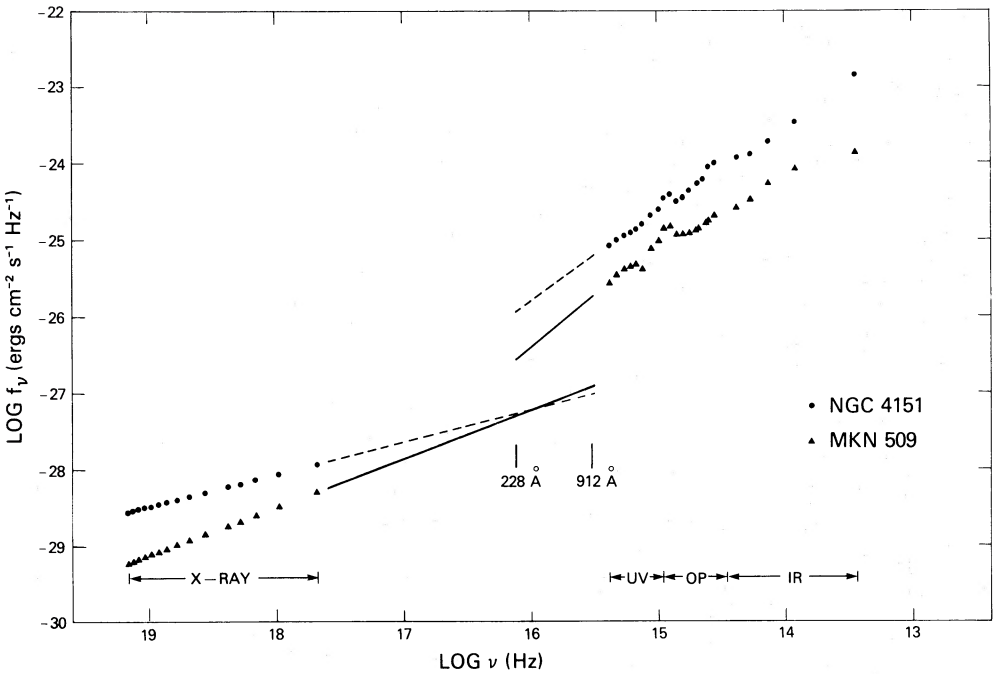

FIG. 4.—The optical–X-ray spectra of two type 1 Seyfert galaxies. The symbols are based on observed values, and the solid and dashed lines are extrapolations. The X-ray spectra are from Mushotzky *et al.* 1980; the IR, optical, and UV are from Rieke 1978, de Bruyn and Sargent 1978, and this investigation, respectively. No correction for reddening has been applied.

spectrum, the optical power law has to turn over and take a steep drop "somewhere." This is consistent with the suggestion by Shuder (1981) who found, from the correlation between the luminosities of Hα and He II λ4686 with that of the nonthermal continuum at 4800 Å, that if one adopts the optical power law to estimate the energy available for heating, then the ionizing continuum needs to be cut off between 60 and 175 eV. *IUE* observations of higher redshift quasars by Green *et al.* (1980) suggest that the turnover of the optical spectrum may already have started around 1100 Å.

b) The Lyα/Hβ *Ratio*

In the previous section we showed the observational evidence that the broad line region of Seyferts and quasars are heated by the photoionization process. But for the composite spectrum of quasars, Baldwin (1977*a*) discovered that the observed Lyα/Hβ ratio is 3, about a factor of 10 lower than that predicted by photoionization models (Davidson 1972; MacAlpine 1972). Similarly low Lyα/Hβ ~ 5 was found by Wu, Boggess, and Gull (1980) for type 1 Seyferts. Some investigators emphasized the effects of dust in lowering the Lyα/Hβ ratio (Netzer and Davidson 1979; Shuder and MacAlpine 1979; London 1979), while others considered the line transfer and collisional excitation and ionization effects (Krolik and McKee 1978; Canfield and Puetter 1981; Kwan and Krolik 1981). Figure 5 is an updated version of the same figure in Wu, Boggess, and Gull (1980); it shows that the observed Lyα/Hβ ratio is about 5. Kwan and Krolik considered the possibility that the excited levels of H I are significantly populated because of the thermalization of Lyα. After the Lyman continuum photons are exhausted at some depth into a broad line cloud, heating by the X-rays maintains a warm region where collisional excitation and ionization from the excited levels occur. Consequently the Balmer lines are enhanced while Lyα is saturated. The Kwan-Krolik model gives Lyα/Hβ ~ 10 without invoking the presence of dust. Our observations show that the 2200 Å dust absorption feature is present in the spectrum of many Seyferts. From the depth of the 2200 Å feature and assuming the average galactic extinction curve of Code *et al.* (1976) to be valid, then $E(B-V) \sim 0.1$ for many galaxies. This leads to another factor of 2 decrease in the Lyα/Hβ ratio. So it seems that the observed Lyα/Hβ ~ 5 can be accounted for by the Kwan-Krolik model and a small amount of extinction along the line of sight. The relatively large $E(B-V) \sim 0.2$–0.4 observed for NGC 7469, 3C 120, and Mrk 79 (Elvius, Lind, and Lindegren 1979; Oke and Zimmerman 1979) is not typical for Seyfert 1 galaxies. However, MacAlpine (1981) pointed out that the contribution of the collisional excitation of Hβ cannot be as large as that suggested by the Kwan-Krolik model; otherwise, the He II λ4686/Hβ ratio will be much smaller than observed. Therefore, he argued that a more important role is played by dust.

In the narrow line region, gas density is $\sim 10^3$–10^6 cm^{-3}, and therefore line transfer effects, which are effective in depressing the Lyα/Hβ ratio, are not important. Netzer (1982) took a fresh look at the Lyα/Hβ

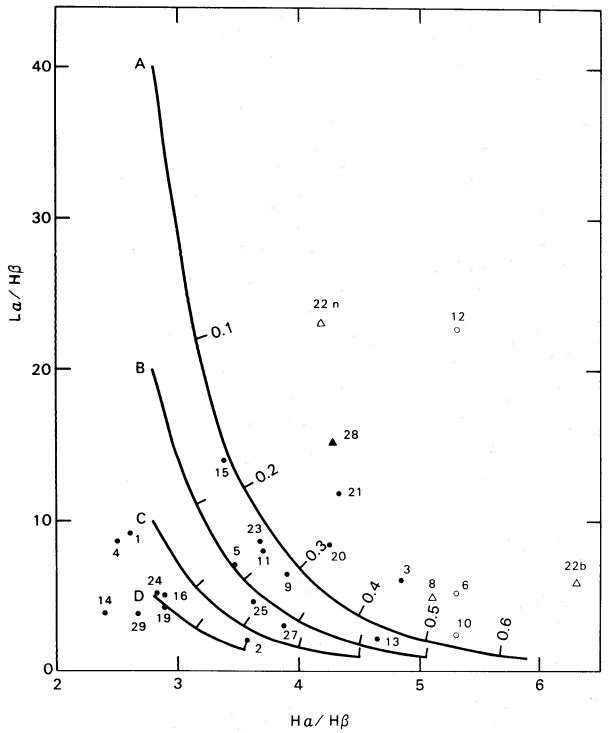

FIG. 5.—The Lyα/Hβ–Hα/Hβ diagram. The symbols have the same meaning as in Fig. 2. The solid curves are the reddening lines based on the extinction curve of Code *et al.* 1976. Curves A, B, C, and D have their origin at Hα/Hβ = 2.8 and Lyα/Hβ = 40, 20, 10, and 5, respectively. Each tick mark indicates an increment of $E(B-V) = 0.1$. The numbers in this figure are the same as the running numbers given in col. (1) of Table 1. For 3C 390.3 (object 22), *n* and *b* are for the narrow and broad components, respectively.

ratio for the narrow line gas. For densities at 10^3–10^6 cm^{-3} and ionization parameter U_1 ($\equiv F_1/hn_e$) $\sim 10^7$ cm s^{-1}, the Lyα/Hβ ratio can be several times higher than the values expected from case B recombination. The recombination values are approached only at the high $U_1 \sim 10^{10}$ cm s^{-1}. The C IV λ1550/C III] λ1909 ratio is a good indicator of U_1 (Davidson 1977). The observed C IV/C III] ratio is 2.5 and 2.3, respectively, for NGC 1068 and Mrk 3. As shown by the extinction curve of Code *et al.* (1976), $E(1550-1909)/E(B-V) = 0.28$. Thus the C IV/C III] ratio is insensitive to reddening. From Figure 1 of Davidson (1977) based on a power-law continuum of $F_\nu \propto \nu^{-1}$, C IV/C III] = 2.5 gives $U_1 \sim 10^8$ cm s^{-1} which is close to the 2×10^8 cm s^{-1} Netzer (1982) found for the narrow line region (NLR) of 3C 390.3. The NLR of 3C 390.3 has been discussed in detail by Netzer; in the following we will be concerned with type 2 Seyferts. Suppose $U_1 \sim 10^8$ cm s^{-1} is typical for Seyfert 2 galaxies; then Netzer's investigation gives the intrinsic Lyα/Hβ ~ 40 and 80, respectively, for $n_e = 2 \times 10^3$ and 2×10^6 cm^{-3}. Figure 5 shows the points for three Seyfert 2 galaxies: NGC 1068 (Lyα/Hβ from Neugebauer *et al.* 1980), Mrk 3, and Mrk 78. Lyα/Hβ = 5.2, 2.3, and 22.6, respectively, for the three objects. The observed ratios are ~2–8 times lower than intrinsic values of Netzer. Comparing with Seyfert 1 galaxies which have observed Lyα/Hβ ~ 5 while the "intrinsic value" of Kwan and Krolik (1981) is 10, Seyfert 2 galaxies may suffer higher reddening by dust. Of course this comparison is highly model dependent and we need to observe more Seyfert 2 galaxies in order to confirm it.

c) Comparison with High Redshift Quasars

i) The Log L_ν(1450) and Log EW (C IV) correlation

In this investigation, we present a homogeneous volume of data on type 1 Seyferts obtained by the *IUE*. There are several sets of data on high *z* quasars measured in a consistent manner with ground-based instruments (e.g., Baldwin 1977*b*; Osmer and Smith 1980); hence, meaningful comparisons can be made between the emission-line properties of high *z* quasars and Seyferts.

Baldwin (1977*b*) searched for luminosity indicators for quasars and found that there was a correlation between the continuum luminosity at 1450 Å and the equivalent width of C IV λ1550. Baldwin's data are plotted in Figure 6 together with the data reported in this investigation, and the data for 3C 273 (Boggess *et al.* 1979), Mrk 205 (measured by the authors), and PKS 0405−123 and PG 0953+415 (Green *et al.* 1980). The data for PKS 1302−102 from Green *et al.* is not plotted because C IV λ1550 falls at 1985 Å, the wavelength region which is near the edge of the SWP camera and at which the LWR camera is insensitive and noisy. Therefore significant uncertainties can be introduced by these instrumental effects. As shown in Figure 6, quasars and BLRG (3C 120 and 3C 390.3) observed by the *IUE* fall in a region defined by or extrapolated from Baldwin's quasars. However, most Seyfert 1 galaxies occupy a region which is below that for the quasars and radio-galaxies. And the C IV equivalent width seems to have reached an upper limit for the low luminosity Seyfert 1 galaxies like NGC 3783, 4151, 4593, and 7213.

One reasonable interpretation for the inverse correlation between the continuum luminosity and the C IV equivalent width—higher luminosity objects have lower C IV equivalent width—is that higher luminosity objects have lower covering factors. There are several lines of evidence which support this interpretation:

1. As will be shown later in this section, the Lyα and C IV equivalent widths for Seyfert 1 galaxies are about a factor of 2 larger than those of high *z* QSOs. This indicates that the broad line region (BLR) of type 1 Seyferts intercepts and absorbs a higher fraction of the available ionizing photons than the BLR of the QSOs.

2. As already pointed out in Peterson *et al.* (1982), the Mg II λ2800 absorption observed in high *z* QSOs occurs at wavelengths well removed from the Mg II emission of the QSOs. Therefore, intergalactic clouds or intervening galaxies, but not the broad line clouds (BLC) of the QSOs, are responsible for the absorption. For Seyfert 1 galaxies, on the other hand, Mg II absorption several angstroms shortward of the emission-line peak is observed in Mrk 279, NGC 5548, and 7469.

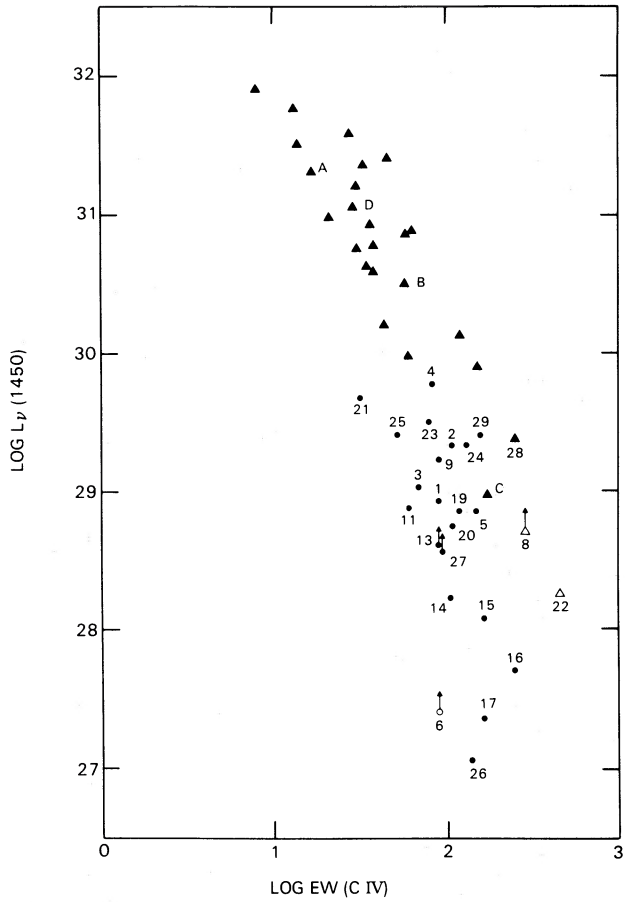

FIG. 6.—The luminosity–equivalent width diagram. The symbols have the same meaning as in Fig. 2. The unidentified filled triangles are the high-redshift quasars from Baldwin 1977*b*; A, B, C, and D are the low-shift quasars as identified in Fig. 3. The numbers are the same as those given in col. (1) of Table 1.

Strong Mg II absorption is also observed in the low luminosity objects NGC 3783, 4151, and probably NGC 4593. In the case of NGC 3783, however, a good fraction of the Mg II absorption originates in our own Galaxy because strong absorption lines of O I λ1304, C II λ1335, and Mg I λ2852 are detected near zero redshift. Incidentally, with the possible exception of NGC 4151, the absorption always occurs shortward of the emission-line peak, indicating that the BLCs are flowing outward.

4. X-ray absorption increases with decreasing luminosity of the active galaxies (Mushotzky 1982). For low luminosity Seyferts, the covering factor approaches unity, and the C IV equivalent width reaches its upper limit.

One may attempt an alternative explanation for this inverse correlation between the continuum luminosity and the C IV equivalent width. Since the resonance lines of abundant ions are expected to have considerable optical thickness, it is conceivable that the emitting clouds for the lower luminosity objects have smaller optical depth and consequently, larger equivalent width, for the C IV line.

Another interesting point in Figure 6 is that the region occupied by the QSOs and BLRGs is above that for Seyfert 1 galaxies. In other words, for the same continuum luminosity, the QSOs and BLRGs have larger C IV equivalent widths. As shown in Figure 2, this is also true for other emission lines. Perhaps radio emission is a manifestation of conditions in some active galactic nuclei which also provide additional heating (e.g., high energy particles). We can speculate on another possibility that there is a disk around the central source. The disk is a continuum source and does not participate in the emission of broad lines (similar to the accretion disk in X-ray binaries and cataclysmic variables). The BLR is outside this disk and it is a spherical ensemble of discrete clouds which are in radial outflow with respect to the central source (Blumenthal and Mathews 1975, 1979; Capriotti, Foltz, and Byard 1980, 1981; Wu, Boggess, and Gull 1981). It is conceivable that, for a given luminosity at 1450 Å, the disk for type 1 Seyferts is more extensive than that for quasars and radio galaxies. Then for Seyferts, a larger fraction of its UV continuum flux is due to thermal emission (the UV excess as discussed in Malkan and Sargent 1982). The larger UV excess leads to a smaller equivalent width for C IV. It is interesting to note that ESO 141−G55 is one of the galaxies which has relatively low L_x/L_ν (1450) ratio (see § III*a*). As reported by Mushotzky *et al.* (1980), its X-ray spectrum has a soft X-ray excess. This soft X-ray component (which does not contribute significantly to the X-ray luminosity) may originate from the inner disk close to the central source, while the outer region of the disk provides sufficient UV excess to bring down the L_x/L_ν (1450) ratio.

ii) *The* Lyα *and* C IV *Equivalent Widths*

Figure 7 gives the histograms for the distribution of the Lyα and C IV λ1550 equivalent widths for quasars and type 1 Seyfert galaxies. The observational data for quasars are obtained from Osmer and Smith (1980), and Table 1 of this paper provides the observed equivalent widths for Seyferts. In Figure 7, the equivalent widths have been corrected for redshift, namely, EW = observed $EW/(1+z)$. It is obvious that, on the average, the Lyα and C IV equivalent widths for type 1 Seyferts are a factor of 2 larger than those for high redshift quasars. As discussed earlier, a reasonable interpretation for this phenomenon is that the covering factor is higher for low luminosity objects.

In a detailed theoretical modeling of NGC 4151, Ferland and Mushotzky (1982, hereafter FM) computed the C IV λ1550 luminosity expected from NGC 4151 if it had a covering factor of unity. As an exercise, we will derive the covering factor for other Seyferts by scaling from the FM results of NGC 4151.

$$P_{\rm CIV}(\text{galaxy}) = P_{42}(\text{N4151}) \times \frac{L_{1450}(\text{galaxy})}{L_{1450}(\text{N4151})} \quad (1)$$

$$\text{Covering Factor} = \frac{L_{\rm CIV}(\text{galaxy})}{P_{\rm CIV}(\text{galaxy})} \quad (2)$$

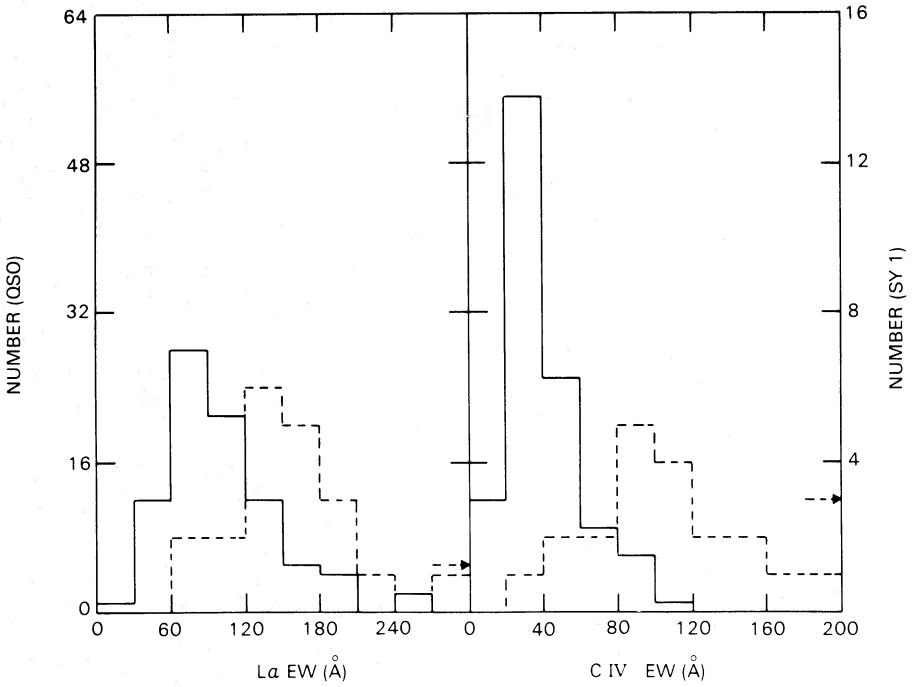

FIG. 7.—The distribution of Lyα and C IV λ1550 equivalent widths for high redshift quasars (*solid histogram*) and type 1 Seyferts and broad line radio galaxies (*dashed histogram*). The arrows indicate the number of objects which have equivalent widths larger than the maximum values given in the graph.

where $P_{\rm C\,IV}$ and P_{42} are the C IV luminosity at 10^{42} ergs s^{-1} expected for covering factor = 1, and L_{1450} and $L_{\rm CIV}$ are the observed continuum luminosity at 1450 Å and the observed C IV luminosity respectively (these quantities are plotted in Fig. 3). NGC 4151 has an I(C IV λ1550)/I(C III] λ1909) = 7.88. We will select those Seyferts with C IV/C III] = 3.5–6.5 and small reddening (i.e., ignoring 3C 120, Mrk 79, and NGC 7469) so as to keep their ionization parameters (see discussion below) similar to that for NGC 4151. As pointed out in § III*a*, the optical–X-ray spectra for type 1 Seyferts are quite similar and with the ionization parameter lie within a small range; it may be reasonable to expect the model for NGC 4151 to be applicable to this selected group of Seyferts. For the low luminosity objects, NGC 3783, 4151, and 4593, equations (1) and (2) give a covering factor of 0.17 ± 0.03,

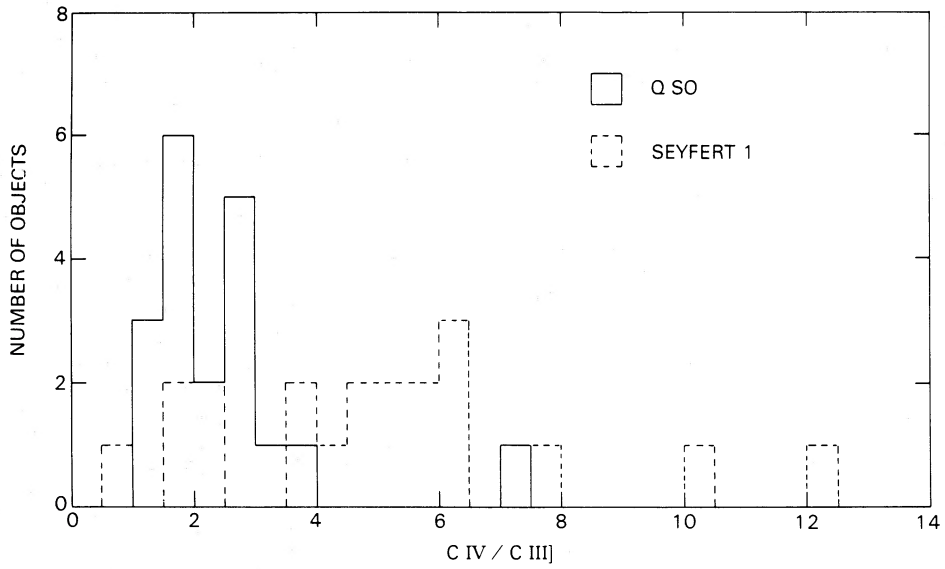

FIG. 8.—The distribution of the intensity ratio between C IV λ1550 and C III] λ1909 for high-redshift quasars and type 1 Seyfert galaxies

while for the nine higher luminosity objects, the covering factor is 0.10 ± 0.03. Indeed, the low luminosity objects have a higher covering factor. Actually, the above average covering facts should be a factor of 2 higher. Because $P_{\rm C\,IV}$ and P_{42} are reddening free, while $L_{\rm C\,IV}$ is the observed value. As mentioned in § III*b*, $E(B-V) \sim 0.1$ for Seyfert 1 galaxies, reddening correction will increase $L_{\rm C\,IV}$ and therefore the covering factor by a factor of 2. Finally, it is interesting to note that equations (1) and (2) give a covering factor of ~ 0.15 for the low luminosity quasars Mrk 205 and MR 2251−178 and ~ 0.05 for the high luminosity quasars PKS 0405−123 and 3C 273, even though the model for NGC 4151 may not be appropriate for the latter two objects because of their low C IV/C III] ratio (~ 2). In summary, this simple exercise shows that the low luminosity objects do indeed have a smaller covering factor.

iii) *The* C IV/C III] *Ratio*

The ionization parameter U_1, in various forms, is used in the theoretical computations of models for active galactic nuclei. It is a quantity which can be used to estimate the ratio between the flux of ionizing photons impinging on a BLC and the electron density of the BLC. For example, $U_1 = F_1/hn_e$, where F_1 is the continuum flux level at the Lyman limit in ergs cm^{-1} s^{-1} Hz^{-1}, h is Planck's constant, and n_e is the electron density. The C IV/C III] ratio is a very sensitive indicator of the ionization parameter (Davidson 1977; Davidson and Netzer 1979; Ferland and Mushotzky 1982). Figure 8 shows the distribution of the C IV/C III] ratio for quasars and Seyferts. Again, the data for high redshift quasars are taken from Osmer and Smith (1980), and Table 1 provides the data for the Seyferts. The high redshift quasars have a C IV/C III] ratio of about 2 while for the type 1 Seyferts, the ratio clusters around 5. From the CNO-rich model in Figure 1 of Davidson (1977), the above C IV/C III] ratios give $U_1 \sim 10^8$ cm s^{-1} for quasars and $U_1 \sim 4 \times 10^8$ cm s^{-1} for type 1 Seyferts. Assuming that the electron density for the broad line clouds are similar in quasars and Seyferts, then $U_1 \propto F_1 \propto L_1 R^{-2}$, where L_1 is the continuum luminosity at the Lyman limit and R is some average radius of the BLR. From Figure 6, we can state that an average quasar is about a factor of 100 brighter than an average type 1 Seyfert. Consequently, the BLR of quasars is on the average 20 times larger than that of type 1 Seyferts.

Again, one may invoke the optical depth effect of C IV λ1550 to explain the observed difference in the C IV/C III] ratio for quasars and type 1 Seyferts. If the emitting clouds of Seyferts have smaller C IV optical depth than quasars, then Seyferts will have higher C IV/C III] ratio as observed. But this explanation is contrary to the conclusions reached from detailed theoretical investigations by Davidson (1977), Davidson and Netzer (1979), and Ferland and Mushotzky (1982). For further discussion, we will continue to adopt that the C IV/C III] ratio is closely linked to the ionization parameter. Bearing in mind, of course, that the critical density for collisional de-excitation of C III] λ1909 is 3×10^9 cm^{-3} (Shuder and MacAlpine 1979), at higher densities, the C IV/C III] ratio may actually increase while U_1 decreases.

As shown in Figure 8, while a good number of the Seyfert 1 galaxies have their C IV/C III] ratio clusters around 5, others have their ratio scattered in a wide range of values. The objects I Zw 1, Mrk 478, II Zw 136, NGC 1566 and 7213 have C IV/C III] $\lesssim 2.3$; the first three of these objects have very strong Fe II emission (Phillips 1977; Osterbrock 1977). Low luminosity Seyferts NGC 4151, Mrk 279, and NGC 3783 have the highest C IV/C III] ratio. Except for NGC 7213, there seems to be a weak correlation between luminosity and the C IV/C III] ratio, in the sense that the ratio is higher for low luminosity objects. For the high redshift quasars the ratio has a smaller range, mostly around 2. For the low redshift quasars, however, PKS 0405−123 and 3C 273 have a ratio of ~ 2, while the low luminosity objects Mrk 205 and MR 2251−178 have 6.2 and 10.8 respectively.

d) Comparison With Model

As shown in Figure 8, there is a concentration of Seyfert galaxies at C IV/C III] ~ 5. They seem to constitute a rather homogeneous group of objects. This is consistent with the discussions given in the previous sections that they have rather similar properties such as the ionization parameter and the $L_x/L_\nu(1450)$ ratio. We will consider the Seyferts having C IV/C III] = 3.5–6.5 to belong in this group and compare their observed line ratios with the recent detailed model computations by Kwan and Krolik (1981). The above range of C IV/C III] ratio gives a range of log $U_1 = 8.4$–8.7 for the CNO-rich model in Figure 1 of Davidson (1977). The standard model of Kwan and Krolik has log $U_1 = 8.95$ (the value for Mrk 279) in Davidson's notation, particle density of 4×10^9 cm^{-3}, and solar abundance for all elements except carbon which is set at a factor of 3.5 lower than the solar value. The Kwan and Krolik model includes ionization and excitation of hydrogen from excited levels and the effects of penetration by hard X-rays beyond the high excitation totally ionized region and create a warm region in the back of a cloud where the low excitation emission lines are produced.

Table 2 shows the comparison between the observed line ratios and those computed by Kwan and Krolik (1981). Three objects which have their dereddened C IV/C III] ratio in the 3.5–6.5 range are not included in Table 2 because of their high reddening; they are 3C 120, Mrk 79, and NGC 7469. The Paα/Hα ratios given in Table 2 are obtained from Lacy *et al.* (1981). The comparison shown in Table 2 indicates that the line ratios computed by Kwan and Krolik (1981) match closely the observed values of this group of galaxies. These galaxies are blue, X-ray bright, large emission line widths, $I(\rm H\beta) \gtrsim I([O\ III])$ and moderate or weak Fe II emission.

NGC 3783, 4151, and Mrk 279 have C IV/C III] = 7.88–12.4; their Lyα/Hβ and Lyα/C IV are slightly lower than the observed mean ratios in Table 2. But except for

TABLE 2

COMPARISON BETWEEN OBSERVED AND COMPUTED LINE RATIOS

Object	C IV/C III]	Lyα/Hβ	Lyα/C IV	Mg II/Hβ	Paα/Hα	Hα/Hβ
Mrk 335	6.34	9.22	2.88	0.44	...	2.60
III Zw 2	3.62	1.92	1.45	0.39	0.13	3.58
Fairall 9	5.04	8.50	2.56	0.89	...	2,51
NGC 985	3.68	6.89	1.42	1.77	...	3.48
Akn 120	5.76	6.41	1.67	1.38	...	3.90
NGC 4593	6.00	...	...	1.06	...	2.61
NGC 5548	5.54	7.87	1.47	1.46	0.10	4.21
ESO 141−G55	4.79	8.67	1.94	1.28	...	3.67
Mrk 509	4.89	5.18	1.67	0.95	0.14	2.83
Mean	5.07	6.83	1.88	1.07	0.12	3.27
Corrected for $E(B-V)=0.1$	5.2	12.4	2.2	1.4	0.10	2.9
Kwan and Krolik model	5.0	10.4	1.6	1.8	0.09	4.2

their high C IV/C III] ratio, all the other ratios agree reasonably well with those computed by Kwan and Krolik. On the other extreme, the low C IV/C III] objects I Zw 1, Mrk 478, and II Zw 136 have high Lyα/C IV ratio and strong Fe II emission. These three objects also have significantly narrower UV emission lines than the objects in Table 2. NGC 1566 and 7213 also have low C IV/C III] ratios; however, other line ratios are not available for comparison.

IV. SUMMARY

New measurements of fluxes and equivalent widths for Lyα, C IV λ1550, C III] λ1909, and Mg II λ2800, and the monochromatic continuum flux at the rest wavelength of 1450 Å are reported for 20 Seyfert galaxies and a low redshift quasar MR 2251−178. Published data are available for nine additional objects. The results and interpretations derived from this volume of data are summarized below:

1. The observed fluxes of Lyα, C IV λ1550, C III] λ1909, and Mg II λ2800 of type 1 Seyfert galaxies correlate well with the observed continuum flux at 1450 Å. The correlations between the C IV luminosity and that at 1450 Å and the 2–10 keV band are good. These results reinforce the hypothesis that photoionization by the nonthermal continuum is the main source of heating for these active galactic nuclei.

2. The optical–X-ray spectra of Seyfert galaxies are very similar to one another. For the 15 type 1 Seyferts which have $E(B-V) \lesssim 0.10$, 12 have the $L_x/L_\nu(1450)$ ratio within a factor of 2 of 1.6×10^{15} Hz.

3. The spectrum between 10 μm and 1200 Å is steeper than that from 2 to 60 keV. In the critical region between the Lyman limit and 2 keV, the extrapolation of the IR-UV spectrum falls significantly above that of the X-rays. Therefore, a simple extrapolation of the optical spectrum may grossly overestimate the amount of ionizing photons.

4. The observed Lyα/Hβ ratio is about 5. After correcting for $E(B-V) \sim 0.1$ (a value suggested by the 2200 Å dust absorption feature observed in an appreciable number of Seyferts), the Lyα/Hβ ratio is approximately 10. This agrees closely with the theoretical value computed by Kwan and Krolik (1981).

5. There is an inverse correlation between the luminosity at 1450 Å and the equivalent width of C IV λ1550 in the sense that lower luminosity objects have higher equivalent width. This is interpreted as an indication that the covering factor increases with decreasing luminosity.

6. The equivalent widths of Lyα and C IV λ1550 at the rest frame of the emitter cluster around 80 Å and 40 Å respectively, for high z quasars and 160 Å and 100 Å for Seyfert 1 galaxies. This suggests that Seyfert 1 galaxies have higher covering factor.

7. The I(C IV λ1550)/I(C III] λ1909) ratio is about 2 for high z quasars and 5 for type 1 Seyferts, indicating that the Seyfert 1 galaxies have a higher ionization parameter than high z quasars.

8. The line ratios predicted by the Kwan and Krolik (1981) model are found to be in good agreement with those observed for type 1 Seyferts with the C IV/C III] ratio between 3.5 and 6.5.

We wish to thank Drs. Gary Ferland, Gordon MacAlpine, Richard Mushotzky, Richard Puetter, and Daniel Weedman for fruitful discussions and Drs. Richard Mushotzky, Donald Osterbrock, and Bradley Peterson for allowing us to use their data in advance of publication. We also wish to thank Mrs. Ruth E. Bradley and Mr. Zoltan G. Levay for their invaluable assistance in data reduction and the staff of the NASA *IUE* Observatory for their help in obtaining and processing our data. C.-C. W. gratefully acknowledges the financial support provided by the NASA *IUE* Project through research contract NAS 5-25774.

REFERENCES

Adams, T. F., and Weedman, D. W. 1975, *Ap. J.*, **199**, 19.
Anderson, K. S. 1970, *Ap. J.*, **162**, 743.
Baldwin, J. A. 1977*a*, *M.N.R.A.S.*, **178**, 67P.
———. 1977*b*, *Ap. J.*, **214**, 679.
Blumenthal, G. R., and Mathews, W. G. 1975, *Ap. J.*, **198**, 517.
———. 1979, *Ap. J.*, **233**, 479.
Boggess, A. *et al.* 1978*a*, *Nature*, **275**, 372.
———. 1978*b*, *Nature*, **275**, 377.

Boggess, A. *et al.* 1979, *Ap. J.* (*Letters*), **230**, L131.
Bohlin, R. C., and Holm, A. V. 1980, *IUE Newsletter No. 10*, p.37.
Bohlin, R. C., Holm, A. V., Savage, B. D., Snijders, M. A. J., and Sparks, W. M. 1980, *Astr. Ap.*, **85**, 1.
Bohlin, R. C., and Snijders, M. A. J. 1978, *IUE Newsletter No. 2*.
Boksenberg, A., Carswell, R. F., Allen, D. A., Fosbury, R. A. E., Penston, M. V., and Sargent, W. L. W. 1977, *M.N.R.A.S.*, **178**, 451.
Canfield, R. C., and Puetter, R. C. 1981, *Ap. J.*, **243**, 390.
Canizares, C. R., McClintock, J. E., and Ricker, G. R. 1978, *Ap. J.* (*Letters*), **226**, L1.
Capriotti, E., Foltz, C., and Byard, P. 1980, *Ap. J.*, **241**, 903.
———. 1981, *Ap. J.*, **245**, 396.
Code, A. D., Davis, J., Bless, R. C., and Hanbury Brown, R., 1976, *Ap. J.*, **203**, 417.
Davidson, K. 1972, *Ap. J.*, **171**, 213.
———. 1977, *Ap. J.*, **218**, 20.
Davidson, K., and Netzer, H. 1979, *Rev. Modern Phys.*, **51**, 715.
de Bruyn, A. G., and Sargent, W. L. W. 1978, *A.J.*, **83**, 1257.
de Bruyn, A. G., and Wilson, A. S. 1976, *Astr. Ap.*, **53**, 93.
Elvius, A., Lind, J., and Lindegren, L. 1979, in *The First Year of the IUE Symposium*, ed. A. J. Willis (London: University College London), p. 119.
Ferland, G. J., and Mushotzky, R. F. 1982, *Ap. J.*, **262**, 564 (FM).
Green, R. F., Pier, J. R., Schmidt, M., Estabrock, F. B., Lane, A. L., and Wahlquist, H. D. 1980, *Ap. J.*, **239**, 483.
Hawley, S. A., and Phillips, M. M. 1978, *Ap. J.*, **225**, 780.
Holm, A. V. 1979, *IUE Newsletter No. 7*, p. 27.
Koski, A. T. 1978, *Ap. J.*, **223**, 56.
Krolik, J. H., and McKee, C. F. 1978, *Ap. J. Suppl.*, **37**, 459.
Kwan, J., and Krolik, J. H. 1981, *Ap. J.*, **250**, 478.
Lacy, J. H., *et al.* 1982, *Ap. J.*, **256**, 75.
Lawrence, A., and Elvis, M. 1982, *Ap. J.*, **256**, 410.
Lewis, D. W., MacAlpine, G. M., and Weedman, D. W. 1979, *Ap. J.*, **233**, 787.
London, R. 1979, *Ap. J.*, **228**, 8.
MacAlpine, G. M. 1972, *Ap. J.*, **175**, 11.
———. 1981, *Ap. J.*, **251**, 465.
MacAlpine, G. M., and Feldman, F. R. 1982, *Ap. J.*, **261**, 412.
MacAlpine, G. M., Williams, G. A., and Lewis, D. W. 1979, *Pub. A.S.P.*, **91**, 746.
Malkan, M. A., and Sargent, W. L. W. 1982, *Ap. J.*, **254**, 22.
Mushotzky, R. F. 1982, *Ap. J.*, **256**, 92.
Mushotzky, R. F., Marshall, F. E., Boldt, E. A., Holt, S. S., and Serlemitsos, P. J. 1980, *Ap. J.*, **235**, 377.
Netzer, H. 1982, *M.N.R.A.S.*, **198**, 589.
Netzer, H., and Davidson, K. 1979, *M.N.R.A.S.*, **187**, 871.
Neugebauer, G., *et al.* 1980, *Ap. J.*, **238**, 502.
Oke, J. B., and Goodrich, R. W. 1981, *Ap. J.*, **243**, 445.
Oke, J. B., and Zimmerman, B. 1979, *Ap. J.* (*Letters*), **231**, L13.
Osmer, P. S., and Smith, M. G. 1980, *Ap. J. Suppl.*, **42**, 333.
Osmer, P. S., Smith, M. G., and Weedman, D. W. 1974, *Ap. J.*, **192**, 279.
Osterbrock, D. E. 1977, *Ap. J.*, **215**, 733.
———. 1978, *Proc. Nat. Acad. Sci.*, **75**, 540.
———. 1980, private communication.
Osterbrock, D. E., and Phillips, M. M. 1977, *Pub. A.S.P.*, **89**, 251.
Osterbrock, D. E., and Shuder, J. M. 1982, *Ap. J. Suppl.*, **49**, 149.
Peterson, B. M. 1982, private communication.
Peterson, B. M., Foltz, C. B., Capriotti, E. R., and Wu, C.-C. 1982, preprint.
Phillips, M. M. 1977, *Ap. J.*, **215**, 746.
Rieke, G. H. 1978, *Ap. J.*, **226**, 550.
Schleicher, H., Fricke, K. J., and Kollatschny, W. 1980, in *Proc. Second European IUE Conference, ESA SP-157*, p. 271.
Shuder, J. M. 1981, *Ap. J.*, **244**, 12.
Shuder, J. M., and MacAlpine, G. M. 1979, *Ap. J.*, **230**, 348.
Snijder, M. A. J., Boksenberg, A., Haskell, J. D. J., Fosbury, R. A. F., and Penston, M. V. 1980, *Proc. Second European IUE Conference, ESA SP-157*, p. 279.
Ward, M. J., Wilson, A. S., Penston, M. V., Elvis, M., Maccacaro, T., and Tritton, K. P. 1978, *Ap. J.*, **223**, 788.
Weedman, D. W. 1977, *Ann. Rev. Astr. Ap.*, **15**, 69.
Wu, C.-C., Boggess, A., and Gull, T. R. 1980, *Ap. J.*, **242**, 14.
———. 1981, *Ap. J.*, **247**, 449.
———. 1982, in preparation.
Zirin, H. 1978, *Ap. J.* (*Letters*), **222**, L105.

A. BOGGESS and T. R. GULL: Code 683, NASA Goddard Space Flight Center, Greenbelt, MD 20771
CHI-CHAO WU: Space Telescope Science Institute–CSC, Homewood Campus, Baltimore, MD 21218